J. Mol. Model. **1999**, *5*, 37 – 45

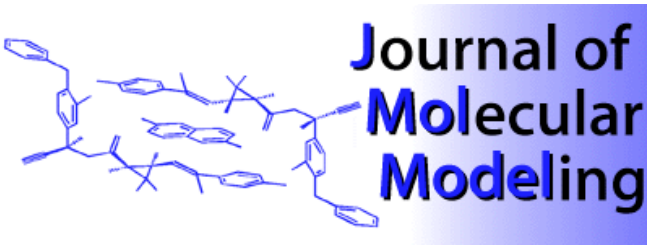

FULL PAPER

Structure-based Reevaluation of the Mechanism of Class I Fructose-1,6-bisphosphate Aldolase

Christophe L.M.J. Verlinde[1] and Paulene M. Quigley[2]

[1]Department of Biological Structure, Biomolecular Structure Center, University of Washington, Box 357742, Seattle, WA 98195, USA. Tel. (206)543 8865; Fax (206)685 7002. E-mail: verlinde@gouda.bmsc.washington.edu

[2]Department of Chemistry, Biomolecular Structure Center, University of Washington, Box 357742, Seattle, WA 98195, USA.

Received: 19 November 1998/ Accepted: 2 February 1999/ Published: 9 March 1999

Abstract The enzymatic reaction carried out by class I fructose-1,6-bisphosphate aldolase is known in great detail in terms of reaction intermediates, but the precise role of individual amino acids in the active site is poorly understood. Therefore, on the basis of the crystallographic structure of the complex between aldolase and dihydroxyacetone phosphate a molecular modelling study was undertaken to predict the Michaelis complex with fructose-1,6-bisphosphate and several covalent enzymatic reaction intermediates. This model reveals the unknown 6-phosphate binding site and assigns distinct roles to crucial residues. Asp33 is responsible for aligning the 2-keto function of the substrate correctly for nucleophilic attack by Lys229, and plays a role in carbinolamine formation. Lys146 assists in carbinolamine dehydration and is essential for stabilising the developing negative charge on O4 of fructose-1,6-bisphosphate during hydroxyl proton abstraction by Glu187. Subsequently, Glu187 is also responsible for protonating C1 of the dihydroxyacetone phosphate enamine. In addition, the absolute configuration of the fructose-1,6-bisphosphate carbinol intermediate is shown to be (*2S*), in agreement with the crystal structure, but opposite from the interpretation in the literature of the stereospecific reduction of the aldolase fructose-1,6-bisphosphate complex with sodium borohydride. It is demonstrated that the outcome of the latter type of experiment critically depends on conformational changes triggered by Schiff base formation.

Keywords Aldolase, Mechanism, Borohydride reduction

Running title Mechanism of class I fructose-1,6-bisphosphate aldolase

Correspondence to: C.L.M.J. Verlinde

Introduction

Despite a plethora of kinetic, mutagenesis and structural experiments on class I fructose-1,6- bisphosphate aldolase [1,2], a full understanding of the catalytic mechanism is limited by the lack of an atomic model of the binding mode of the substrate fructose-1,6-bisphosphate (Fru-1,6-P_2). The precise role of the various amino acid residues in the active site is especially controversial [2-4]. Recently, the structure of a Michaelis complex between the rabbit muscle enzyme and the product dihydroxyacetone phosphate (DHAP) at 1.9 Å has become available [5]. Here, we will show that this structure is the key to further insight into the enzymatic mechanism via molecular modelling studies.

Fructose-1,6-bisphosphate aldolase (EC 4.1.2.13) catalyzes the reversible cleavage of fructose- 1,6-bisphosphate into glyceraldehyde-3-phosphate (G3P) and dihydroxyacetone phosphate (DHAP), and is thus important in glycolysis and gluconeogenesis. It can also cleave fructose-1-phosphate, which is of significance in fructose metabolism. Two types of aldolases can be distinguished. Class I aldolases, mainly present in higher eukaryotes, are homotetramers. They form a covalent imine intermediate with the substrate during catalysis, and are the subject of this paper. Class II aldolases, mainly present in eubacteria, require Zn^{2+} or sometimes Fe^{2+}. Though vertebrates have three class I aldolase isoenzymes, called A, B and C, all are believed to employ the same catalytic mechanism [2].

The currently accepted mechanism of class I fructose-1,6-bisphosphate aldolase has largely been derived from kinetic studies. It consists of the following seven steps shown schematically in Figure 1 (all residue numbers in this paper refer to the rabbit muscle enzyme):

(i) the β-furanose form of Fru-1,6-P_2, 81 % of the isomeric species in solution [6],undergoes ring opening when bound to the enzyme [7]; (ii) Lys229 carries out a nucleophilic attack on the carbonyl of Fru-1,6-P_2 [8,9], and forms a transient carbinolamine [10,11]; (iii) the carbinolamine undergoes dehydration, yielding the Schiff base (imine) of Fru-1,6-P_2 [12]; (iv) a proton is abstracted from the 4-hydroxyl, after which the C3-C4 bond is broken and the enamine of

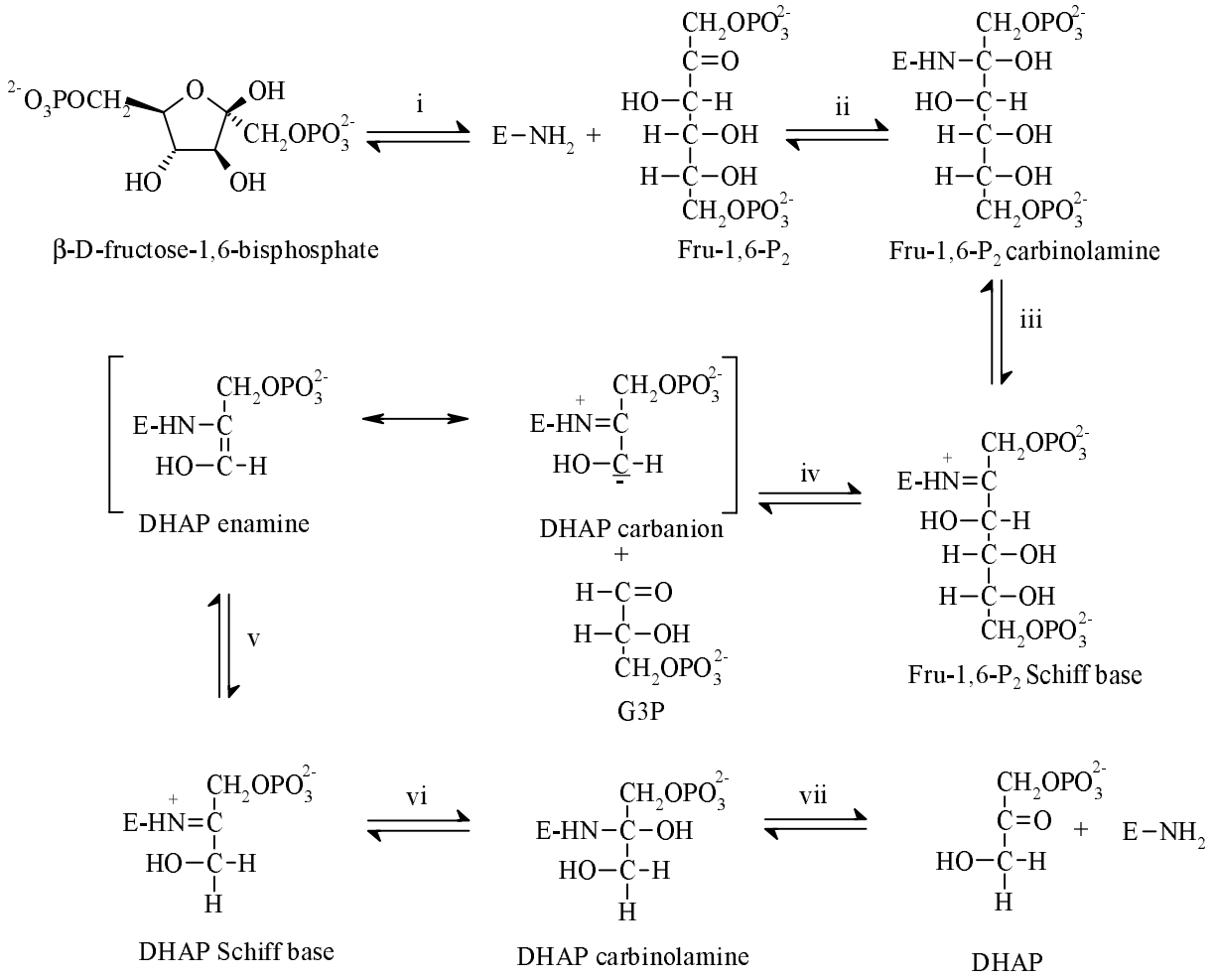

Figure 1 *Mechanism of class I fructose-1,6-bisphosphate aldolase*

DHAP is formed [13,14]; (v) glyceraldehyde-3-phosphate (G3P) is released, and the enzyme protonates the enamine, forming the Schiff base of DHAP [15]; (vi) water attacks the Schiff base and a carbinolamine is formed [10]; (vii) the bond with the Lys 229 amine breaks, DHAP is formed and released from the enzyme [11]. Besides the undisputed Lys 229, several residues have been implicated in this mechanism, but their roles are subject to multiple possible interpretations in the absence of a structural model. On the basis of mutation studies, Asp 33 was put forward as the base responsible for proton abstraction in step 4 [16], but so was the C-terminus Tyr 363 [3]. Chemical inactivation studies led to suggestions that Lys 107 might interact with the 6-phosphate of Fru-1,6-P_2 [17,18], while Arg 52 [19] and Arg 148 might recognise the 1-phosphate [20]. On the grounds of mutational studies, Lys 146 appears to be important, but not less than five possible roles have been suggested for it [3,4,21]. Also, Glu 187 is crucial for catalysis [22], but evidence for its proposed role in carbinol dehydration is circumstantial. It appears thus that the catalytic mechanism is well understood in terms of substrate intermediates but not in terms of the enzyme.

Various crystal structures have shed some light on the catalytic mechanism. Thus far, the three-dimensional structures of rabbit muscle [5,23], human muscle [24], *Drosophila melanogaster* [25] and *Plasmodium falciparum* aldolase [26] have been reported. Each of the enzyme monomers is a classical $(\beta\alpha)_8$ barrel with the implicated catalytic residues positioned fairly deeply in the centre. The C^{α} traces of all structures superimpose within 1.5 Å r.m.s. deviation when the C-terminal tail of the enzyme is excluded from the comparison [26]. These last 20 residues adopt widely divergent conformations, even between different monomers of the same enzyme. The crystal structures have put to rest early claims [1] that Cys residues are involved in catalysis as there are none in the active site; moreover, the implicated residues are not conserved. Thus far, only one catalytically relevant molecule has been observed in the active site of aldolase, the cleavage product DHAP [5]. It was observed in three binding modes, which all share the same phosphate moiety locus. Only in one of the binding modes does C2 come within contact of the N^{ζ} of K229, making it a likely candidate for the Michaelis complex. This structure is an excellent starting point to examine the catalytic mechanism of aldolase by molecular modelling.

Molecular modelling

Throughout this paper the atomic numbering of Fru-1,6-P_2 has been transferred to DHAP to facilitate discussion. Adhering to nomenclature rules would lead to confusion since C1 of Fru-1,6-P_2 is equivalent to C3 of DHAP, and *vice versa*.

The Michaelis complex between aldolase and DHAP [5] exhibits the following interactions (Figure 2): (i) the phosphate is sequestered by three protein backbone nitrogens, of Ser 271, Gly 272 and Gly 302; the latter residue is at the N-terminus of a helix, characteristic for phosphate binding sites [27]; the phosphate is also a hydrogen bond donor to the carbonyl of Ser 300, consistent with evidence that the enzyme prefers a mono anion at that site [28]; (ii) C1 and C2 are in hydrophobic contact with the side chain of Ala 31; C2 is also at 3.1 Å from the N^{ζ} of Lys 229, the residue responsible for forming the Schiff base; (iii) the keto oxygen O2 is 2.8 Å from both N^{ζ} of Lys 146 and $O^{\delta 1}$ of Asp 33; the latter implies that Asp 33 is protonated, in agreement with its position in a partially hydrophobic environment at the bottom of the enzyme barrel ($O^{\delta 1}$ at 3.7 Å from Ala 31 and 3.9 Å from Ile 71;

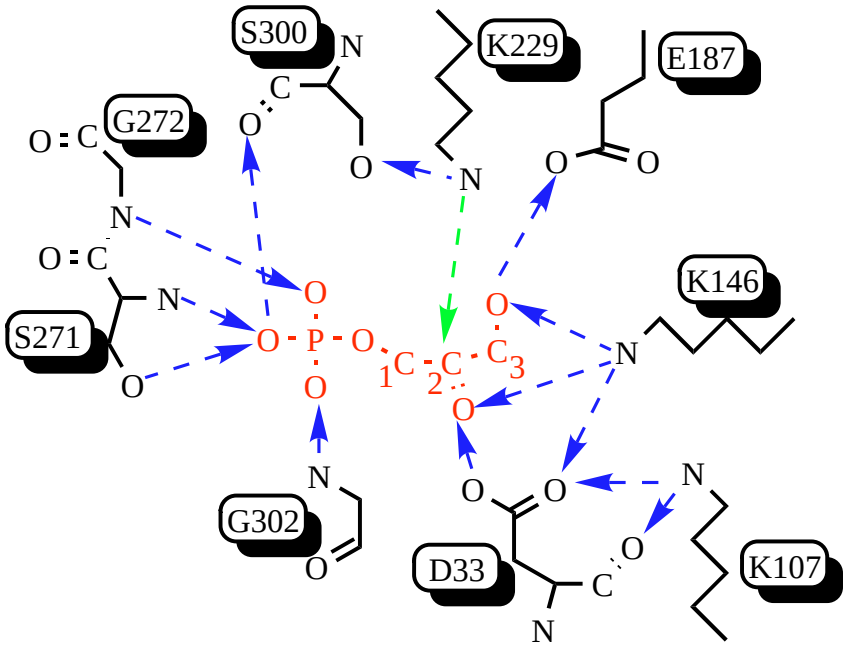

Figure 2 *Crystallographically observed interactions between DHAP and aldolase. Hydrogen bonds are dashed arrows with the head towards the acceptor. The incipient nucleophile, Lys 229, is at 3.1 Å from DHAP's C2 (green arrow). Coordinates from PDB entry 1ADO [5] were used to determine the interactions*

$O^{\delta 2}$ at 4.2 Å from Ile 71); (iv) the O3 hydroxyl hydrogen bonds with Lys 146 and Glu 187. Our starting hypothesis was that all of the observed interactions of DHAP would be maintained in the Michaelis complex with Fru-1,6-P_2.

Three different and independent approaches were taken to model the Fru-1,6-P_2 binding mode. First, Fru-1,6-P_2 was grown atom-by-atom in the enzyme binding site starting from the crystallographically observed DHAP coordinates using the molecular modelling package BIOGRAF [29] in conjunction with the Dreiding force-field [30] under default conditions. After each atom addition a full conformational search about the newly formed torsion angle was carried out in steps of 10°, local minima were optimised and further subjected to atom-by-atom growth. Branches of the growth process that led to unresolvable clashes with the protein, even by local protein relaxation, were pruned. An example of such a branch is the one that maintains the C1-C2-C3-O3 torsion angle of 101° observed for DHAP: it leads to serious clashes between C4 and the side chains of Lys 146, Glu 187 and Lys 229. Eventually, this growth process resulted in seven potential binding models for Fru-1,6-P_2 that were examined; their interaction energies were: -2, -24, -35, -36, -37, -39 and -80 kcal/mol. Only two models exhibited substantial coordination of the 6-phosphate, and both put the 6-phosphate in the

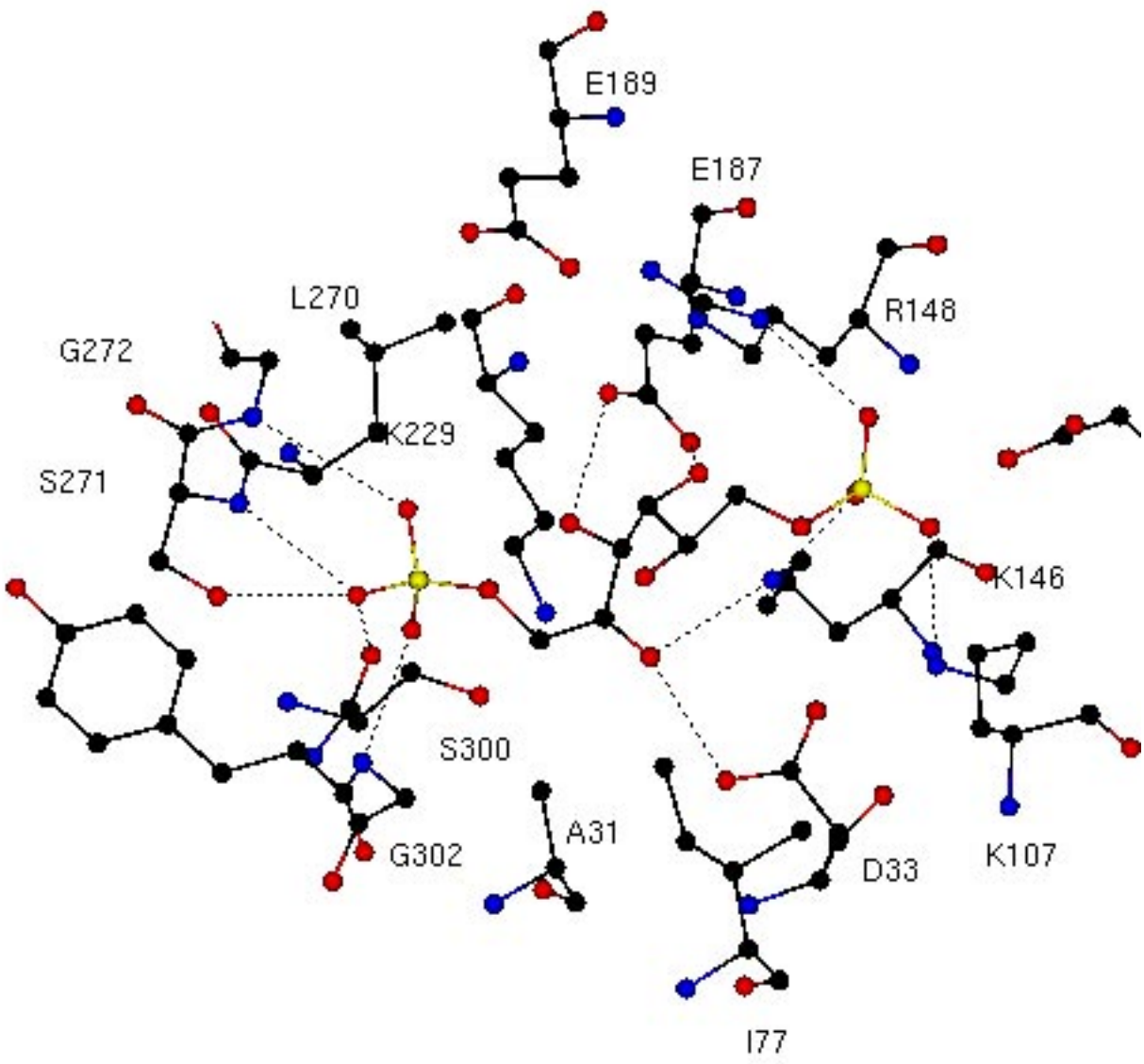

Figure 3a *Proposed binding mode of fructose-1,6-bisphosphate to aldolase. VRML scene with hydrogen bonds in green lines; drawn with MOLSCRIPT [43]*

same locus. One of the two corresponded to the global minimum at -80 kcal/mol and was therefore considered to correspond to the Michaelis complex.

Second, Fru-1,6-P_2 was docked into the binding site by an extensive Monte Carlo search procedure implemented in the program QXP; 1,000 cycles were run [31]. QXP uses a different force-field than BIOGRAF, and the Monte Carlo method does not suffer from a preset torsional increment, an obvious limitation of the first procedure. The 1-phosphate and the carbonyl positions were tethered to their experimentally observed positions within 0.5 Å while the rest of the molecule was subjected to the search procedure. All suggested docking modes put the 6-phosphate approximately in the same position. The lowest energy one was identical to the BIOGRAF solution.

Third, the preferential positions for the 1- and 6-phosphates of Fru-1,6-P_2 were examined with the GRID program [32] using the PO4H and PO4 probes, representative for a mono and dianion, respectively. With both probes two preferential sites were found in the active site, one corresponding to the experimentally observed 1-phosphate position (PO4H: -19.2 kcal/mol; PO4: -16.8 kcal/mol) and a second one near Lys 107, Lys 146 and Arg 148 (PO4H: -18.0 kcal/mol; PO4: -16.5 kcal/mol). Gratifyingly, the 6-phosphate position coincides with the one suggested in the first two docking approaches.

Binding mode of fructose-1,6-bisphosphate

The proposed binding mode of Fru-1,6-bisphosphate to aldolase is shown in Figure 3. From the 1-phosphate up to the 2 keto functionality atoms occupy the positions seen in the DHAP complex. However, the O3 hydroxyl adopts a different orientation. It still makes a hydrogen bond with Glu 187 but has lost the one with Lys 146. The O4 hydroxyl also interacts with Glu 187, while the O5 hydroxyl points into solvent. Experimentally, O5 has been shown to be dispensable as the Km of 5-deoxy-fructose-1,6-bisphosphate is 20 times tighter than of Fru-1,6-bisphosphate, while Vmax is 2.7 times faster [6]. The 6-phosphate is involved in three salt bridges. Thus, each polar atom of Fru-1,6-P_2 except for O5 makes a direct interaction with the protein. All of the residues implicated in binding are absolutely conserved between the 33 fructose-1,6-bisphosphate class I aldolase sequences present in the SWISSPROT sequence databank.

Proposal for the enzyme mechanism

The proposed binding mode of Fru-1,6-P_2 forms a good starting point to gain further insight into the catalytic mechanism. For that purpose, using the BIOGRAF modelling package, we modelled several of the subsequent covalent reaction intermediates: the Fru-1,6-P_2 carbinolamine, the Fru-1,6-P_2 Schiff base, the DHAP enamine, the DHAP Schiff base and the DHAP carbinolamine. All residues in the binding site were kept fixed except for the side chain of Lys 229, the incipient nucleophile. The results of these docking studies will be discussed as we proceed systematically through the reaction.

Opening of the Fru-1,6-P_2 β-furanose isomer

Despite a rate of ring opening in solution for the β-isomer of Fru-1,6-P_2 that is nearly as fast as kcat of the aldolase reaction [6], there are indications that ring opening occurs after

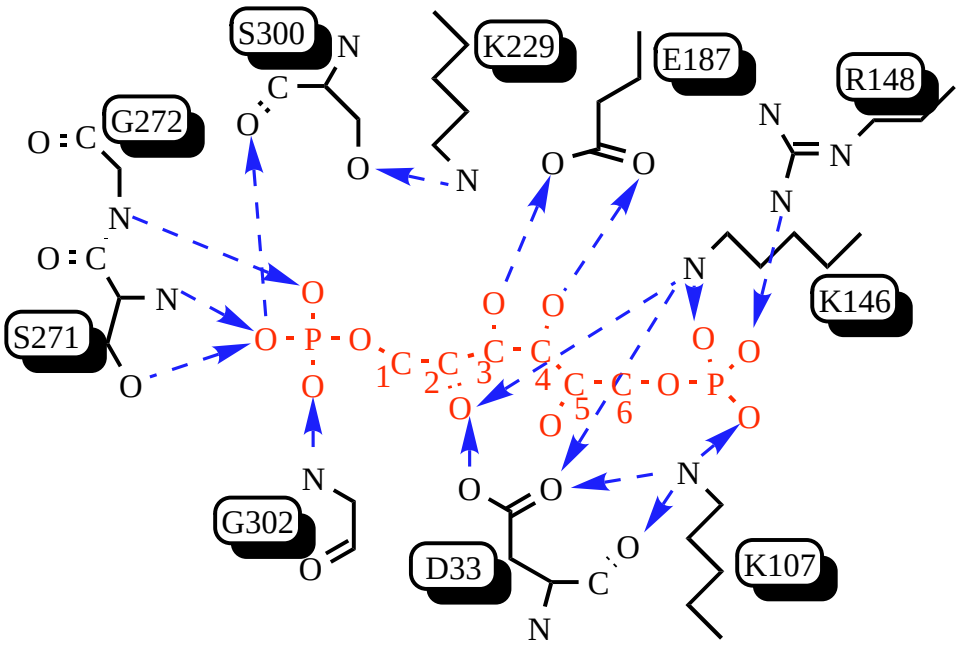

Figure 3b *Proposed binding mode of fructose-1,6-bisphosphate to aldolase. Schematic representation of the binding mode*

binding to the enzyme [7]. This possibility was therefore examined. In the modelled acyclic conformation of Fru-1,6-P_2 the C2 and O5 atoms are only 3.3 Å apart. Due to this close proximity it was straightforward to model the cyclic form of the substrate in the active site of the enzyme. The assumption that the O2 atom would not move much automatically led to a β-furanose isomer model. The r.m.s. deviation between the docked acyclic and cyclic forms was only 0.2 Å when O5 was omitted from the calculation. The proximity of Lys 146 to the furanose ring oxygen suggests that the enzyme might assist ring opening by acid catalysis.

Attack by the nucleophile Lys 229

Lys 229 can only be a nucleophile if it is uncharged. In the crystal structure with DHAP it makes one hydrogen bond, with O^{Γ} of Ser 300, and is in contact with C^{β} of Ala 31 (3.9 Å), $C^{\delta 1}$ of Ile 77 (4.1 Å), and O1 (3.4 Å), C1 (3.6 Å) and C2 (3.1 Å) of DHAP. This partially hydrophobic environment might account for a sufficiently lowered pK_a of Lys 229 to lose a proton. The proton must be lost to a solvent molecule as the closest base, the Glu 187 carboxylate, is 3.9 Å away. The angle formed between the incipient nucleophile and the

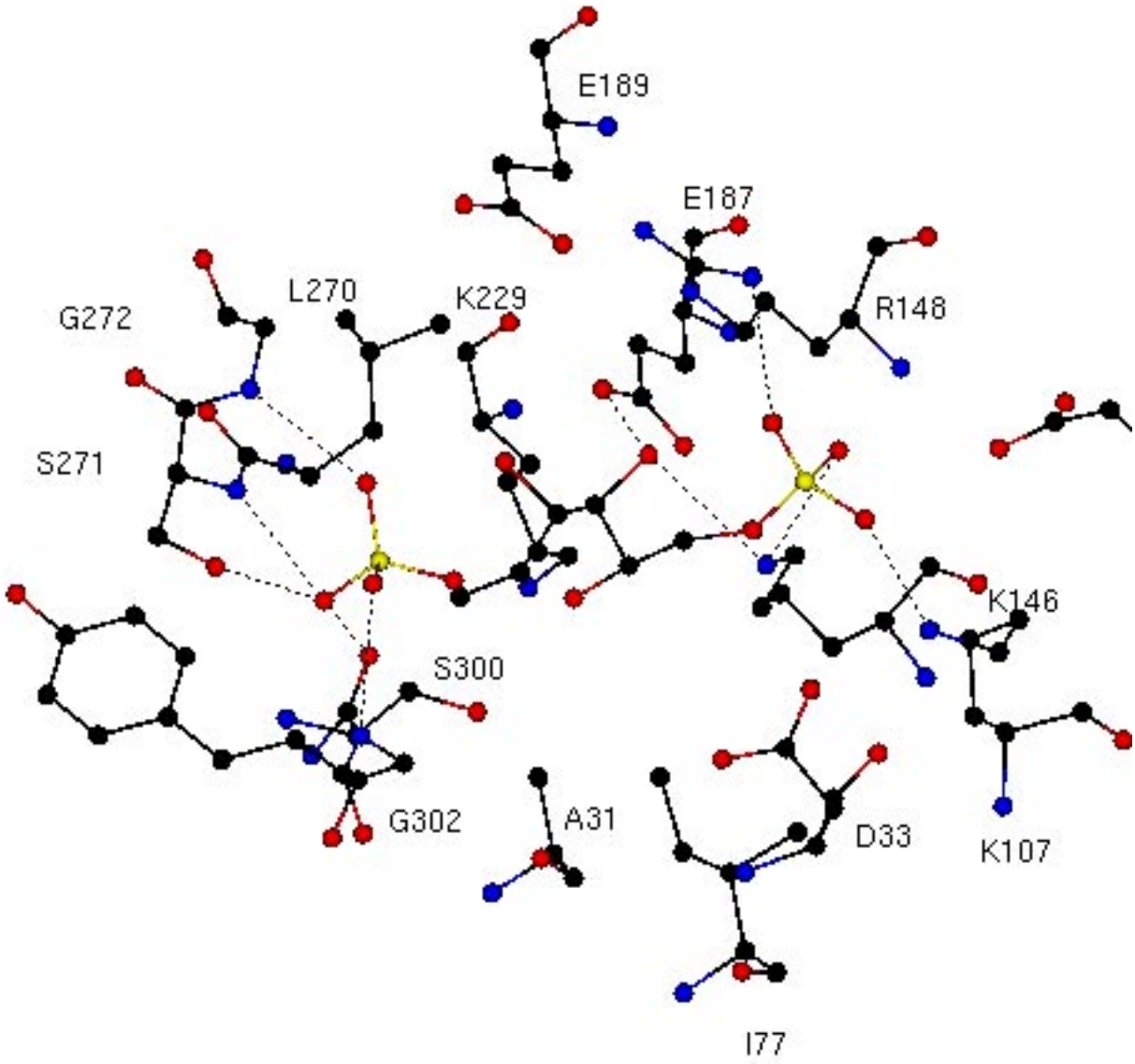

Figure 4 *Binding mode of the Fru-1,6-P_2 Schiff base. The O4 hydroxyl is perfectly poised for proton abstraction by Glu 187 and is also making a hydrogen bond to Lys 146. Hydrogen bonds are given in green lines; drawn by MOLSCRIPT [43]*

Table 1 *Properties of aldolase mutants [a]*

Mutant	Relative Km (Fru-1,6-P_2)	Relative V_{max} (Fru-1,6-P_2) steps: i→vii [b]	Relative carbanion formation from Fru-1,6-P_2 steps: i→ii→iii→iv [b]	Relative carbanion formation from DHAP steps: vii→vi→v→iv [b]
D33A	6	1/5,500	1/131	1/5
D33S	3	1/3700	ND [c]	ND
D33E	7	1/900	1/22	1/17
K146A	ND	<1/100,000	1/304	1/143
K146L	ND	<1/100,000	1/406	1/8
K146Q	ND	<1/100,000	1/609	1/77
K146H	32	1/2,500	1/406	1/4
K146R	1	1/500	1/244	1/125
E187Q	ND	1/25,000	ND	ND

[a] All numbers are relative to the wild type enzyme, i.e. mutant / wt
[b] steps refer to figure 1
[c] ND = not determined

substrate carbonyl, N^{ζ} ... C2=O2, is 94°. According to Bürgi et al., the transition state of a nucleophilic addition reaction exhibits an angle between 100 and 110° [33]. Therefore, Lys 229 is in an ideal position for a nucleophilic attack, which results in the formation of a carbinolamine.

Formation of the Fru-1,6-P_2 carbinolamine

Carbinolamine formation can occur by at least two routes: (i) concerted addition of amine and protonation of the carbonyl oxygen; or (ii) formation of a zwitterion followed by protonation [34]. Given the availability of protons to O2 *via* its hydrogen bond partners, Asp 33 and Lys 146, is seems likely that the first route is taken by the enzyme. This poses a dilemma as to whether Asp 33 or Lys 146 donates the proton. If it is Asp, then its hydrogen bonds to Lys 107 and Lys 146 become salt bridges, which should be energetically favourable. If it is Lys, then its salt bridge to the 6-phosphate is lost. Therefore, it appears logical that Asp 33 donates a proton to O2. The presence of the nearby Lys 146 might help stabilise the developing negative charge on O2 during the nucleophilic addition. Subsequently, the N-protonated species loses quickly a proton, with a rate constant of up to 108 and a pKa of 2 [35], probably to a solvent molecule as the closest base, Glu 187, is 4.3 Å away.

From Figure 3 it is obvious that Lys 229 attacks C2 of the substrate from the *re* face to form a *(2S)*-carbinolamine and eventually a Schiff base. This is contrary to the interpretation of an experiment by DiIasio et al. [36]. After sodium borohydride reduction followed by protein hydrolysis they only found glucitollysine, not the epimer mannitollysine, which indicates that the *re* face of the Schiff base is exposed to the reducing agent in the solvent. Therefore, they assumed that the Lys had been attacking the opposite face of the substrate carbonyl, the *si* face. However, molecular modelling of the Schiff base shows that upon forming a covalent bond C2 moves by 2.0 Å towards the Lys N^{ζ}, and importantly, that the plane of the sp2 centre rotates by 66° compared to the noncovalent complex. As a result, the *si* face of C2, which was solvent exposed before the nucleophilic attack, becomes completely buried by Leu 270 (Figure 4), as is obvious from molecular surface calculations with BIOGRAF. Concomitantly, the *re* face, which was originally buried and faced Lys, becomes exposed to the borohydride in the solvent, in agreement with the production of glucitollysine in the experiment.

Dehydration of the carbinolamine into the Schiff base

Carbinolamine dehydration is the second step in the formation of a Schiff base from a carbonyl compound and an amine. At a pH above 6.0 this elimination is subject to both general base and acid catalysis [37,38]. In the modelled carbinolamine (not shown) only Lys 146 is within hydrogen bond distance of the carbinol O2. Hence, acid assisted catalysis by that residue is likely, making the alcohol a much better leaving group. Subsequently, Lys 146 could quickly recapture a proton from the solvent, perhaps the one lost from the N-protonated carbinolamine species. Dehydration of the carbinolamine yields a cationic Schiff base, which acts as an electron sink in the cleavage reaction.

Proton abstraction from O4 by Glu 187 followed by C3-C4 cleavage

After formation of the Schiff base the 4-hydroxyl of the substrate is perfectly aligned for proton abstraction towards the *syn* lone pair of the $O^{\varepsilon 2}$ from Glu 187 (Figure 4). It has been suggested that the *syn* orientation of a carboxylate is sub-

stantially more favourable for proton transfer than *anti* [39]. Glu 187 sits at the bottom of the enzyme barrel and is mostly buried between the aliphatic portions of the Lys 229 and Arg 148 side chains. This might raise its pK_a and facilitate proton abstraction. Remarkably, O4 is at 3.0 Å from N^{ζ} of Lys 146, suggesting that this residue might play an essential role in polarising the O4 hydroxyl for proton abstraction by Glu 187 and in stabilising the developing negative charge. After removal of the O4 proton the C3-C4 bond becomes unstable and breaks, producing the enamine of DHAP and glyceraldehyde-3-phosphate, which is released.

Protonation of the DHAP enamine

Another resonance form of the DHAP enamine is the ketimine, with C3 as a carbanion. Therefore, it is not a surprise that C3 is prone to protonation. Careful titration experiments indicate that the proton donor has a pKa of 5.2 [40]. The models of the DHAP enamine and ketimine show only one proton donor close enough to C3 (at 3.1 Å), namely the earlier protonated Glu 187 (not shown). The orientation of the proton is consistent with stereospecific exchange of the *pro-(S)* proton at C3 of DHAP [41]. For some aldolase isoenzymes the C-terminal Tyr residue improves the efficiency of this step. For example, C-terminally truncated or mutated rabbit and human muscle aldolase exhibit a 20-fold lower overall reaction rate as compared to wild type enzyme, an effect which has been traced to reduced enamine protonation [13,42]. Unfortunately, in most crystal structures the C-terminal tail of the enzyme adopts a conformation far away from the active site. Only in the human muscle aldolase crystal structure does the Tyr point into the active site. However, that conformation is likely to be catalytically incompetent as the Tyr phenol function occupies the 1-phosphate position of the substrate. In view of the lack of structural information and the enzyme's ability to proceed with catalysis without the C-terminal Tyr, we refrain from speculating on the precise interactions this residue makes with the DHAP enamine enzyme complex.

Formation of the DHAP carbinolamine

Our modelling suggests that the hydrolysis of the DHAP Schiff base proceeds *via* a carbinolamine, likely *via* the reverse steps of the Fru-1,6-P_2 Schiff base formation.

Active site mutants and the mechanism

Several active site mutants of Asp 33, Lys 146 and Glu 187 have been made to probe the catalytic mechanism of aldolase [4,16,21,22]. Their properties are summarised in Table 1, and the following discussion requires careful consideration of the enzymatic reaction steps depicted in Figure 1.

The impaired carbanion formation by Asp 33 mutants, either from Fru-1,6-P_2 or DHAP, can be explained by a reduced efficiency of any step of the enzymatic reaction leading up to the carbanion. Morris and Tolan proposed that Asp 33 might be responsible for proton abstraction from the O4 hydroxyl [16]. However, this hypothesis is difficult to reconcile with the facts that substantial levels of carbanion are formed from Fru-1,6-P_2, and that processing of DHAP in the reverse enzymatic reaction is affected. In our proposed mechanism Asp 33 is required for efficient carbinolamine formation, or the reverse step, the second part of Schiff base hydrolysis. Obviously, impaired carbinolamine formation automatically leads to reduced levels of carbanion intermediates from both Fru-1,6-P_2 and DHAP. In addition, Asp 33 also ensures the correct orientation of the 2-keto group of the substrate.

Lys 146 mutants are devoid of catalytic power with Fru-1,6-P_2 as a substrate except if they retain a positively charged residue at that position [4,21]. In contrast their capability to form the carbanion of DHAP is retained. Hence, the justified conclusion by Morris and Tolan [21] that Lys 146 must play a crucial role in Fru-1,6-P_2 cleavage. This agrees perfectly with our proposed mechanism in which Lys 146 serves to stabilise the developing negative charge on O4 during proton abstraction. Lys 146 also may aid in carbinolamine dehydration.

Glu 187 mutants are largely inactive, but they have only been characterised in terms of the overall enzymatic reaction [22]. The dramatic loss of activity is in agreement with our proposed role of this residue in proton abstraction from O4 and protonation of the DHAP enamine.

Conclusion

The prediction of the Michaelis complex between aldolase and fructose-1,6-bisphosphate and the different covalent reaction intermediates for the first time clearly define the roles of the individual amino acids in the active site. Major findings are the location of the 6-phosphate binding site, the roles of Asp 33 and Lys 146 in Schiff base formation, the function of Lys to lower the pKa of the substrate's O4 hydroxyl, and the double role of Glu 187 in O4 hydroxyl proton abstraction and DHAP enamine protonation. We hope that the proposed enzyme mechanism will provide the necessary structural framework for experimentalists to determine the pK_a of the large number of amines and carboxylates in the active site of aldolase.

Acknowledgments We would like to thank Dr. Erkang Fan for insightful discussions and Dr. Ellie Adman for critically reading the manuscript.

Supplementary Material available Figure 3a and figure 4 are available in VRML format. This format allows for interactive inspection of the 3D-models by use of standard HTML/VRML browsers.

Note added in print During submission of this manuscript two groups deposited coordinates with the PDB for the experimental structure of aldolase in complex with F1,6–BP. The entry codes of the, as yet not released, coordinates are: 4ALD and 6ALD (marked for release upon publication).

References

1. Horecker, B.L.; Tsolas O.; Lai, C.Y. *Enzymes (3rd ed.)* **1972**, *VII*, 213-258.
2. Gefflaut, T.; Blonski, C.; Perié, J.; Willson, M. *Prog. Biophys. Molec. Biol.* **1995**, *63*, 301-340.
3. Littlechild, J.A.; Watson, H.C. *Trends Biochem. Sci.* **1993**, *18*, 36-39.
4. Morris, A.J.; Davenport, R.C.; Tolan, D.R. *Prot. Eng.* **1996**, *9*, 61-67.
5. Blom, N.; Sygusch, J. *Nature Struct. Biol.* **1997**, *4*, 36-39.
6. Midelfort , C.F.; Gupta, R.K.; Rose, I.A. *Biochem.* **1976**, *15*, 2178-2185.
7. Rose, I.A.; O'Connell, E.L. *J. Biol. Chem.* **1977**, *252*, 479-482.
8. Grazi, E.; Rowley, P.T.; Cheng, T.; Tchola, O.; Horecker, B.L. *Biochem. Biophys. Res. Comm.* **1962**, *9*, 38-43.
9. Lai, C.Y.; Nakai, N.; Chang, D. *Science* **1974**, *183*, 1204-1206.
10. Ray, B.D.; Harper, E.T.; Fife, W.K. *J. Am. Chem. Soc.* **1983**, *105*, 3731-3732.
11. Rose I.A.; Warms J.V. *Biochem.* **1985**, *24*, 3952-3957.
12. Avigad, G.; Englard, S. *Arch. Biochem. Biophys.* **1972**, *153*, 337-346.
13. Rose, I.A.; O'Connell, E.L.; Mehler, A.H. *J. Biol. Chem.* **1965**, *240*, 1758-1765.
14. Healy, M.J.; Christen, P. *Biochem.* **1973**, *12*, 35-41.
15. Kuo, D.J.; Rose, I.A. *Biochem.* **1985**, *24*, 3947-3952.
16. Morris, A.J.; Tolan, D.R. *J. Biol. Chem.* **1993**, *268*, 1095-1100.
17. Shapiro, S.; Enser M., Pugh, E.; Horecker, B.L. *Arch. Biochem. Biophys.* **1968**, *128*, 554-562.
18. Anai, M.; Lai, C.Y.; Horecker, B.L. *Arch. Biochem. Biophys.* **1973**, *156*, 712-719.
19. Patthy, L.; V'aradi, A.; Th'esz, J.; Kov'acs, K. *Eur. J. Biochem.* **1979**, *99*, 309-313.
20. Lobb, R.R.; Stokes, A.M.; Hill, H.A.; Riordan, J.F. *Eur. J. Biochem.* **1976**, *70*, 517-522.
21. Morris, A.J.; Tolan, D.R. *Biochem.* **1994**, *33*, 12291-12297.
22. Blonski, C.; De Moissac, D.; Perié, J.; Sygush, J. *Biochem. J.* **1997**, *323*, 71-77.
23. Sygusch, J.; Beaudry, D.; Allaire, M. *Proc. Natl. Acad. Sci. USA* **1987**, *84*, 7846-7850.
24. Gamblin, S.J.; Davies, G.J.; Grimes, J.M.; Jackson, R.M.; Littlechild, J.A.; Watson, H.C. *J. Mol. Biol.* **1991**, *219*, 573-576.
25. Hester, G.; Brenner-Holzach, O.; Rossi, F.A.; Struck-Donatz, M.; Winterhalter, K.H.; Smit, J.D.; Piontek, K. *FEBS Lett.* **1991**, *292*, 237-242.
26. Kim, H.; Hol, W.G.J. *J. Mol. Biol.* **1998**, *278*, 5-11.
27. Hol, W.G.J.; van Duijnen, P.T.; Berendsen, H.J.C. *Nature* **1978**, *273*, 443-446.
28. Grazi, E.; Sivieri-Pecorari ,C.; Gagliano, R.; Trombetta, G. *Biochem.* **1973**, *12*, 2583-2590.
29. BIOGRAF version 3.21 **1993**, Molecular Simulations, San Diego, CA 92121, USA.
30. Mayo, S.L.; Olafson, B.D.; Goddard III, W.A. *J. Phys. Chem.* **1990**, *94*, 8897-8909.
31. McMartin, C.; Bohacek, R.S. *J. Comput.-Aided Mol. Des.* **1997**, *11*, 333-344.
32. Goodford, P.J. *J. Med. Chem.* **1985**, *28*, 849-857.
33. Bürgi, H.B.; Dunitz, J.D.; Lehn, J.M.; Wipff, G. *Tetrahedron* **1974**, *30*, 1563-1572.
34. Sayer, J.M.; Pinsky, B.; Schonbrunn, A.; Washtien, W. *J. Am. Chem. Soc.* **1974**, *96*, 7998-8009.
35. Rosenberg, S.; Silver, S.M.; Sayer, J.M.; Jencks, W.P. *J. Am. Chem. Soc.* **1974**, *96*, 7986-7998.
36. DiIasio, A.; Trombetta, G.; Grazi, E. *FEBS Lett.* **1977**, *73*, 244-246.
37. Sayer, J.M.; Peskin, M., Jencks, W.P. *J. Am. Chem. Soc.* **1973**, *95*, 4277-4287.
38. Sayer, J.M.; Jencks, W.P. *J. Am. Chem. Soc.* **1977**, *99*, 464-474.
39. Gandour, R.D. *Bioorg. Chem.* **1981**, *10*, 169-176.
40. Rose, I.A.; Warms, J.V.; Kuo, D.J. *J. Biol. Chem.* **1987**, *262*, 692-701.
41. Rieder, S.V.; Rose, I.A. *J. Biol. Chem.* **1959**, *234*, 1007-1011.
42. Takahashi, I.; Takahashi, Y.; Hori, K. *J. Biochem.* **1989**, *105*, 281-286.
43. Kraulis, P.J. *J. Appl. Crystallogr.* **1991**, *24*, 946-950.